

2009

Tokai to Kamioka: A 2nd Generation Long Baseline Neutrino Experiment

Jessica Danielle Brinson

Follow this and additional works at: https://digitalcommons.lsu.edu/honors_etd



Part of the [Astrophysics and Astronomy Commons](#)

Tokai to Kamioka: A 2nd Generation Long Baseline Neutrino Experiment

by

Jessica Brinson

Undergraduate Honors Thesis under Direction of

Dr. Thomas Kutter

Department of Physics and Astronomy

Submitted to the LSU Honors College in Partial Fulfillment of

the Upper Division Honors Program

December 2009

Louisiana State University

Agricultural and Mechanical College

Baton Rouge, Louisiana

Table of Contents

1. Neutrinos.....	3
2. Neutrino Interactions.....	4
3. Neutrino Oscillations.....	4
4. T2K Experiment.....	6
5. T2K Neutrino Production.....	9
6. Neutrino Interaction Vertices.....	13
7. Detector Interactions.....	16
8. Muon Neutrino Disappearance.....	16
9. Electron Neutrino Appearance.....	19
10. Electron Neutrino Background	22
11. Extracting θ_{13} and Δm^2_{23}	24
12. Summary.....	26
13. Conclusion.....	27

List of Figures

1. Neutrinos

Figure 1.1: Standard Model of Particle Physics.....	3
---	---

3. Neutrino Oscillations

Figure 3.1: PMNS Mixing Matrix (3 neutrinos).....	5
---	---

Figure 3.2: PMNS Mixing Matrix (2 neutrinos).....	5
---	---

4. T2K Experiment

Figure 4.1: General Layout of T2K Experiment.....	7
---	---

Figure 4.2: On and Off Axis Near Detectors for T2K.....	7
---	---

Figure 4.3: Far Detector for T2K.....	8
---------------------------------------	---

Figure 4.4: Muon and Electron Ring Events at Super K.....	9
---	---

5. Neutrino Production

Figure 5.1: Energy Spectra of All Neutrinos for Near and Far Detectors.....	10
---	----

Figure 5.2: Ratio of Energy Spectrum at ND280 to that of Super K (no oscillations).....	11
---	----

Figure 5.3: Energy Spectra According to Neutrino Type for Near and Far Detectors.....	11
---	----

Figure 5.4: Energy Spectra According to Parent Particle for Near and Far Detectors.....	12
---	----

6. Neutrino Interaction Vertices

Figure 6.1: Neutrino Interaction Vertices in Near Detector.....	14
---	----

Figure 6.2: Ratio of All Events in Near Detector to Events at Center.....	15
---	----

Figure 6.3: Illustration of Position of Near Detector.....	15
--	----

8. Muon Neutrino Disappearance

Figure 8.1: Energy Spectra with Muon Neutrino Disappearance.....	17
--	----

Figure 8.2: Energy Spectra with Muon Neutrino Disappearance (vary $\sin^2 2\theta_{23}$).....	18
--	----

Figure 8.3: Energy Spectra with Muon Neutrino Disappearance (vary Δm^2_{23}).....	19
--	----

9. Electron Neutrino Appearance

Figure 9.1: Energy Spectrum with Electron Neutrino Appearance.....	20
--	----

Figure 9.2: Energy Spectra with Electron Neutrino Appearance (vary $\sin^2 2\theta_{13}$).....	21
---	----

Figure 9.3: Energy Spectra with Electron Neutrino Appearance (vary Δm^2_{23}).....	21
---	----

10. Electron Neutrino Background

Figure 10.1: Energy Spectra of Electron Neutrinos According to Parent Particle for Near and Far Detectors.....	23
--	----

Figure 10.2: Energy Spectra of muon neutrinos, intrinsic electron neutrinos, and electron neutrinos expected from oscillations.....	23
---	----

11. Extracting θ_{13} and Δm^2_{23}

Figure 11.1: Plot showing the best fit for θ_{13} and Δm^2_{23}	25
--	----

12. Summary

Table 12.1: Event Estimations for Super K.....	27
--	----

1. Neutrinos

A neutrino is a small, almost massless particle that lacks electric charge and travels close to the speed of light. Currently, there are three known flavors of neutrinos. Each flavor has a corresponding lepton partner to which it is associated. The electron neutrino is associated with the electron, the muon neutrino with the muon, and the tau neutrino with the tau [1]. These 6 particles constitute the portion of the Standard Model known as leptons (Fig 1.1).

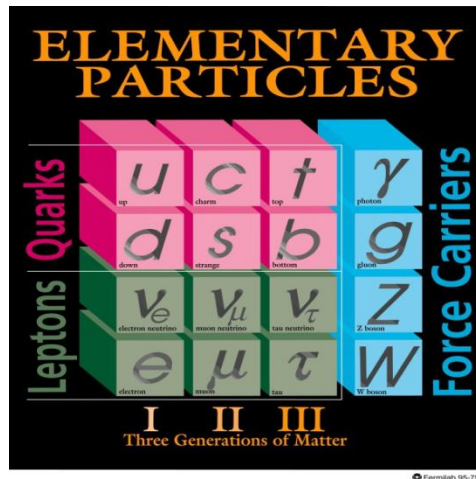


Fig 1.1: An illustration showing the standard model of particle physics

The neutrino was first postulated to exist in 1930 by Wolfgang Pauli. He said that it had to be present in order to account for the conservation of energy in beta decay (the decay of a neutron into a proton, an electron, and as we know today, an antineutrino). In 1956, Cowan and Reines devised an experiment that actually allowed for neutrinos to be detected. They used a nuclear reactor as a source of neutrinos and observed the subsequent interactions of the neutrinos with the protons in water. These interactions produced neutrons and positrons; these product particles could be detected by scintillators and photo-multiplier tubes. In 1962, Lederman, Schwartz, and Steinberger discovered that there was in fact more than one type of neutrino by detecting muon type neutrinos. This trio of scientists used an alternating gradient synchrotron to create a beam of pions (the parent particles of muon neutrinos), which then collided into a steel wall 70 feet from the detector. Muon neutrinos could travel through this wall and then passed into a spark chamber filled with neon gas, creating muons. The sparks that the muons made when they collided with aluminum plates in the neon-filled chamber were photographed, thus proving the existence of muon neutrinos [1]. Then, in the 1970's, the Stanford Linear Accelerator (SLAC) discovered a new particle known as tau. It was hypothesized that it too would have a neutrino partner, but only in the year of 2000 was the DONUT experiment at Fermilab able to verify this. The tau neutrino was the last particle to be added to the Standard Model [8].

2. Neutrino Interactions

Neutrinos can only be detected through their interactions with other materials. However, since they only interact through the weak force (and gravity, but this is negligible on laboratory scales), oftentimes they will fly straight through the detector. The weak interaction affects all left handed leptons and quarks. It is the only interaction capable of changing flavor and violates CP symmetry. It is mediated by the exchange of heavy gauge bosons (W and Z). The W and Z bosons are the carrier particles for the weak force, much like the photon is the carrier particle for the electromagnetic force (see Figure 1.1). In the domain of the weak force, there are two types of interactions that can be observed. The first is a charged current interaction (CC), which can change the generation of the particle involved. The charged current interactions can be subdivided into charged current inelastic and charged current quasi-elastic. The inelastic CC interaction is a reaction in which all new particles are created. The particles that go into the reaction are not the same as the particles that come out of the reaction.

The other type of CC interaction, charged current quasi-elastic (CCQE) involves a neutrino emitting/absorbing a charged W boson and being converted into the corresponding charged lepton (muon, electron, or tau). CCQE interactions are useful because the knowledge of the resulting charged lepton allows us to extract the best information about the neutrino energy spectrum.

The other set of neutrino interactions are the neutral current interactions, in which a lepton can emit or absorb a neutral Z boson. Neutral current interactions allow for elastic scattering of neutrinos in matter. In elastic scattering, the particles that go into the reaction are the same as those which come out. On the other hand, neutral current interactions are also capable of producing other particles. However, in all cases the neutrino remains unchanged, which allows for the detection of neutrinos without their changing into another type of particle [13].

3. Neutrino Oscillations

Once it was discovered that neutrinos existed and were able to be detected from their interactions with other materials, experimentalists had to devise ways to study their properties. However, certain discrepancies were observed. In the 1960's, there were some problems when it came to accurately measuring the flux of electron neutrinos from the sun. It was found that the number of electron neutrinos from the sun that were detected was roughly 1/3 the number that had been predicted by the Standard Solar Model. This became known as the solar neutrino problem and remained a large puzzle for many years. Then, in 1968, Pontecorvo predicted that if the neutrinos were to have mass, they would be able to change into different flavors as they traveled from the Sun to the Earth. Neutrino oscillations would account for this discrepancy between what was seen experimentally and what had been predicted. In 2001, SNO (Sudbury Neutrino Observatory) was able to measure all types of neutrinos that came from the sun and distinguish among the various types. SNO did this by using heavy water in the detector, making it sensitive to a neutral current reaction that has an equal probability of involving any of the three neutrino flavors. SNO found that about 35% percent of the neutrinos that came from the sun were electron

neutrinos, whereas the rest were muon and tau neutrinos. The total number of neutrinos reaching the Earth from the Sun agreed with earlier predictions that were based on nuclear physics and fusion reactions within the sun [9].

The resolution of the solar neutrino problem opened up a whole new field of neutrino physics. Now it was up to experimentalists to uncover how neutrinos oscillated. Pontecorvo predicted that neutrino oscillations are due to a difference in the flavor and mass eigenstates of the neutrino [13]. This relationship is

$$|\nu_i\rangle = \sum_{\alpha} U_{\alpha i} |\nu_{\alpha}\rangle$$

where $|\nu_{\alpha}\rangle$ is a neutrino with definite flavor: $\alpha = e$ (electron), μ (muon) or τ (tau), and $|\nu_i\rangle$ is a neutrino with definite mass: $i = 1, 2$, or 3 . $U_{\alpha i}$ is known as the Pontecorvo-Maki-Nakagawa-Sakata matrix (PMNS matrix). If this were the identity matrix, the mass and flavor eigenstates would be equal as it is for the lepton partners associated with the neutrinos (i.e. the electron, muon, and tau particles). Experiments have shown that this is not the case with neutrinos [11].

$$\begin{bmatrix} 1 & 0 & 0 \\ 0 & c_{23} & s_{23} \\ 0 & -s_{23} & c_{23} \end{bmatrix} \begin{bmatrix} c_{13} & 0 & s_{13}e^{-i\delta} \\ 0 & 1 & 0 \\ -s_{13}e^{i\delta} & 0 & c_{13} \end{bmatrix} \begin{bmatrix} c_{12} & s_{12} & 0 \\ -s_{12} & c_{12} & 0 \\ 0 & 0 & 1 \end{bmatrix} \begin{bmatrix} e^{i\alpha_1/2} & 0 & 0 \\ 0 & e^{i\alpha_2/2} & 0 \\ 0 & 0 & 1 \end{bmatrix}$$

Figure 3.1: PMNS matrix where $c_{ij} = \cos\theta_{ij}$ and $s_{ij} = \sin\theta_{ij}$. θ_{ij} is the mixing angle between the mass and flavor eigenstates i and j . The phase factor δ is non-zero only if neutrinos violate CP symmetry.

Figure 3.1 shows the PMNS matrix. It has been used to derive and describe the probability that a neutrino will oscillate into another, assuming that all three flavors of neutrinos participate in the mixing.

On the other hand, several cases exist where only two types of neutrinos participate significantly in the mixing. If this is the case, the PMNS matrix can be simplified.

$$U = \begin{pmatrix} \cos\theta & \sin\theta \\ -\sin\theta & \cos\theta \end{pmatrix}$$

Figure 3.2: The PMNS matrix if only two neutrinos significantly participate in the mixing, where θ represents the mixing angle of interest.

There are two types of neutrino experiments that are used to study the oscillation parameters of neutrinos. An experiment can either look for the deficit of a type of neutrino or look for the appearance of a new one. Tokai to Kamioka will utilize both of these methods in order to put finer limits on certain parameters of the PMNS matrix [5].

The following equation represents the approximate probability that a muon neutrino will remain a muon neutrino, also known as the muon neutrino survival probability. This can be derived using the PMNS matrix that assumes only two neutrinos participate in the mixing. Since we are only concerned with the fact that a muon neutrino is no longer a muon neutrino, it is safe to assume the electron neutrino and tau neutrino are one type, namely “another” neutrino. This will be used by T2K in order to place better limits on θ_{23} and Δm^2_{23} . The approximate probability formula for muon neutrino survival is

$$P(\nu_\mu \rightarrow \nu_\mu) = 1 - \sin^2 2\theta_{23} \sin^2(1.27\Delta m^2_{23}L/E).$$

The next equation represents the approximate probability that a muon neutrino will oscillate into an electron neutrino. This equation must be derived from the PMNS matrix that assumes all three neutrinos participate in the mixing [2]. This is one of the major goals of T2K and will help measure θ_{13} . The probability formula for electron neutrino appearance is

$$P(\nu_\mu \rightarrow \nu_e) = \sin^2 \theta_{23} \sin^2 2\theta_{13} \sin^2(1.27\Delta m^2_{23}L/E).$$

In both probability formulas, L is the distance traveled by the neutrino, E is the energy of the neutrino, Δm^2_{23} is the difference of the masses squared, θ_{23} is related to the mixing of the muon neutrino, and θ_{13} is related to the oscillation of a muon neutrino into an electron neutrino [5].

It can be seen that both probability formulas have a dependence on L/E , indicating that T2K will have to accurately measure the neutrino energy in order to correctly determine these parameters.

4. T2K experiment

Tokai to Kamioka (T2K) is a second generation long baseline neutrino experiment designed to measure the oscillation parameters of neutrinos. The primary goal of T2K is to search for the oscillation between muon neutrinos (ν_μ) and electron neutrinos (ν_e), thus measuring θ_{13} . θ_{13} is a parameter in the PMNS matrix related to the probability that ν_μ will morph into a ν_e (see Figure 3.1). If θ_{13} does turn out to be nonzero, the second phase of the T2K experiment would be geared towards measuring CP violation in the leptonic sector. CP violation is characterized by the parameter δ (see Figure 3.1) and could give an explanation as to why there is more matter than antimatter in the universe. Another physics goal of T2K includes a precision measurement of the muon neutrino disappearance parameters of θ_{23} and Δm^2_{23} [5].

J-PARC (Japan Proton Accelerator Research Complex) is where the neutrino source, a 50 GeV proton synchrotron is located. Once the proton beam is extracted onto a graphite target, a beam of pions and kaons, the parent particles of neutrinos, is produced. Once this beam of particles leaves the target, it is then focused by a series of three magnetic horns and directed down a decay tunnel which is 110 m long. As the particles travel down the decay tunnel, these pions and kaons will decay into neutrinos which can be detected by near and far detectors. At the end of the decay tunnel there is dirt, which acts as an absorber, ensuring that only neutrinos are in the beam.



Fig 4.1: A diagram showing the general layout of the T2K experiment

It is important to have both a near and far detector in order to accurately study neutrino properties. Since neutrinos oscillate as they travel over distance, it is essential to be familiar with the original composition of the beam. The purpose of the near detector is to measure the initial composition and properties of the beam before any oscillations have taken place. The far detector is responsible for measuring the composition and properties of the beam after it has propagated 295 kilometers. Projections based on what is seen in the near detector are then made for what the beam composition will be when it reaches Super K assuming no oscillations have occurred. When the actual beam composition at Super K is examined (with oscillations), then neutrino oscillations can be observed and studied [5].

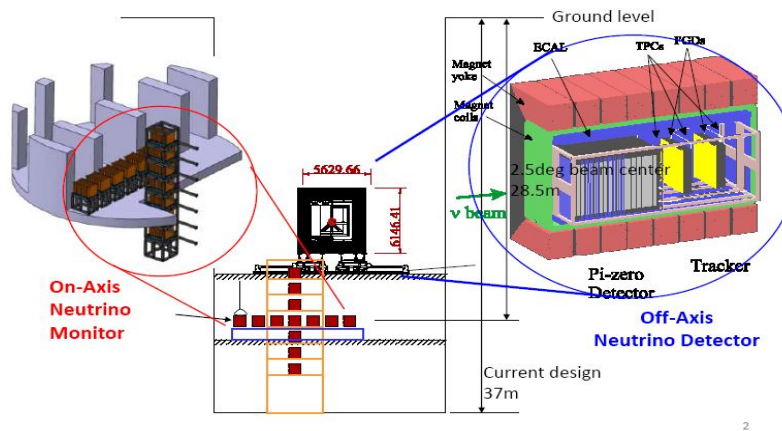


Fig 4.2: The on axis (INGRID) and off axis (ND280) detectors for T2K

There are two near detectors for T2K. One near detector (INGRID) is located on axis (centered with respect to the original beam) and is responsible for monitoring the beam direction, since the beam has the ability to vary between 2 and 3 degrees off axis. However, INGRID is mainly responsible for monitoring the beam profile [5].

The off axis detector (ND280) is located 2.5 degrees off axis with respect to the center of the original beam and is responsible for measuring the neutrino energy spectrum and electron

neutrino background. The off axis detector consists of 5 subdetectors: The Pi Zero Detector (POD), Fine Grained Detector (FGD), the Time Projection Chamber (TPC), and the Electromagnetic Calorimeter (ECal). The purpose of the POD subdetector is to measure the interactions of π^0 's with the water in the detector. There are two FGD's which will produce charged particles through CCQE interactions. There are three TPC's in ND280 which are responsible for tracking the path of these charged particles. This data will be used to measure the neutrino energy spectrum. The ECal will be used to detect the photons that result from the decay of the π^0 's. The last component of ND280 is the Side Muon Range Detector (SMRD). SMRD will contribute to the measurements of the neutrino energy spectrum, trigger on cosmic ray muons for calibration, and identify backgrounds through the use of scintillators embedded into the iron yokes of the magnets in which the central subdetectors are located. A scintillator is made from a substance which can be used to convert the energy of a charged, high energy particle into light. Then the wavelength of this light is shifted (usually into the visible range) by a wavelength shifting fiber running through the scintillator. At the ends of the fiber are photosensors which have been tuned to detect this wavelength of light [6].

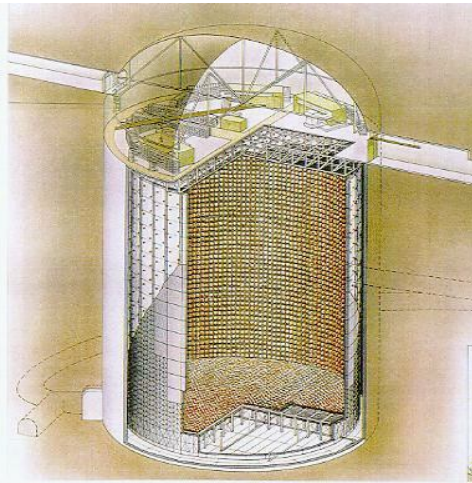


Figure 4.3: An illustration depicting the far detector

The far detector (Super Kamiokande or Super K) is located 295 kilometers from the target and is also off axis by 2.5 degrees. The far detector will use a phenomenon known as Cherenkov radiation to detect neutrinos. When a neutrino collides with the water in Super K, it imparts its momentum to a particle and can accelerate it up to a speed that is greater than the speed of light in that medium. Subsequently, a cone of blue light known as Cherenkov radiation is created and detected by photo-multiplier tubes (PMT's) that line the walls of Super K. Different interactions cause different patterns. These differences can be seen from the readout of the PMT's and will reveal if the incoming neutrino was a muon neutrino or an electron neutrino [5].

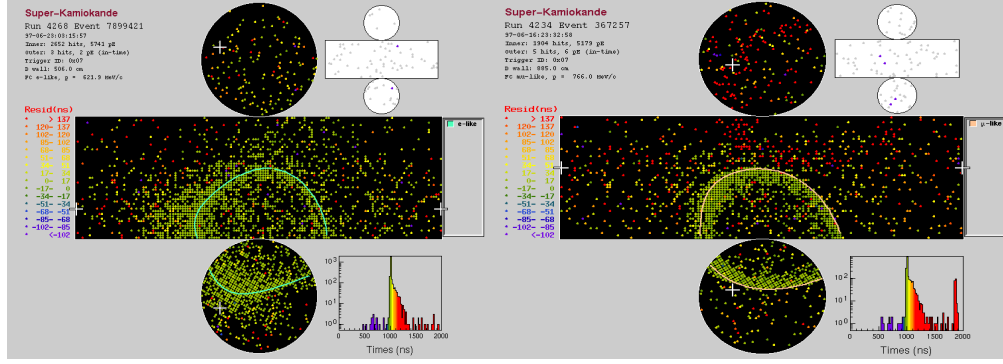


Figure 4.4: Actual event readouts from PMT's in Super K. Electron neutrino event (left), and muon neutrino event (right).

Figure 4.4 reveals the differences in events as seen by Super K. The electron neutrino event is more diffuse because the electron is such a light particle ($mc^2=0.000511$ GeV); it will scatter more causing the picture to be less clear. In contrast, the muon ($mc^2=0.106$ GeV) is 200 times heavier than the electron and will scatter less, revealing a more pronounced ring structure in the PMT's.

The previous four sections of my thesis have been introduction. The remaining nine sections contain the original work that I have done. The goals of my thesis were to study the composition of the beam at ND280 and Super K using simulated data sets, determine the dominant sources of electron neutrino background, and estimate their strength. I studied the neutrino interaction vertices in ND280 as well as the number of interactions that are expected to occur after 5 years of running. In addition, I determined the number of events associated with muon neutrino disappearance and electron neutrino appearance. Lastly, I showed how these parameters are extracted. The remainder of my thesis has been structured in order to address these goals.

I did this through the use of flux files which simulate all neutrinos that impinge upon either detector [14]. All plots made correspond to allowing the beam to run at full intensity for 5 years with the maximum proton energy of 50 GeV. I also used software that simulated the interactions that are expected in ND280.

5. T2K Neutrino Production

T2K produces neutrinos by smashing protons into a graphite target to produce pions and kaons. These pions and kaons then decay into neutrinos. Pions largely prefer to decay into muon neutrinos; therefore, the majority of electron neutrinos that are seen in the original beam are from the decay of kaons.

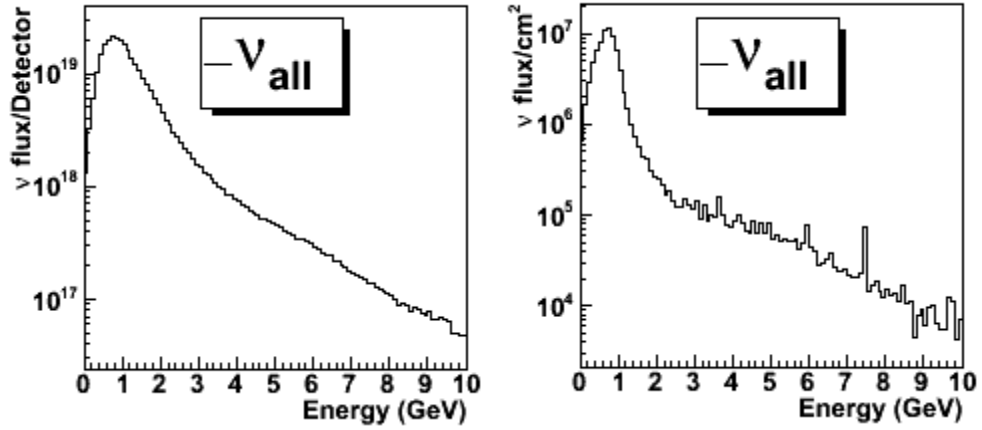


Figure 5.1: Expected energy spectrum of all neutrinos at ND280 (left) and Super K (right). These spectra were made using Monte Carlo simulations. They have been normalized to 5×10^{21} POT (protons on target), which corresponds to running the beam for 5 years at full intensity with the maximum proton energy (50 GeV), and represent all neutrinos that impinge upon either detector.

Figure 5.1 reveals that the energy spectra for the near and far detectors are comparable except for the fact that Super K sees fewer events than the near detector. Since one of the main functions of the near detector is to help estimate what the neutrino flux will be at the far detector, it is important that the spectra be similar. It can be seen that the energy of the neutrinos is narrowly peaked in the lower energy range, a result of T2K's attention to off axis. Having a detector off axis allows for the exploitation of pion decay kinematics to enhance the yield of neutrinos within a specific energy range. The neutrino energy is not closely dependent on the pion energy for a fixed decay angle. Therefore, a broad range of pion energy will yield a highly peaked neutrino spectrum if off axis decays at a particular angle are observed [4]. This peak in the lower energy range is also desirable because the oscillation probability formulas have a dependence on L and E . The distance L is fixed at 295 kilometers or 280 meters; respectively, there must be a narrow range of neutrino energies in order to place reasonable limits on θ_{13} . However, these spectra do have a tail that extends into areas of higher energies. The majority of these events result from kaon decay.

Figure 5.2 shows the ratio of the energy spectrum at Super K to the energy spectrum at ND280. Plots such as these will be essential when creating a model for the far detector (assuming no oscillations) based on information that is gathered in the near detector. In the simplest of cases, the energy spectrum that is measured at ND280 is multiplied by the ratio plot (created using simulations) in order to produce an expected energy spectrum for Super K.

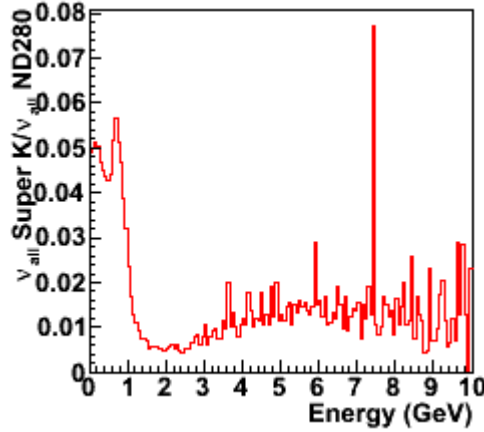


Figure 5.2: Ratio of the energy spectrum of Super K to the energy spectrum of ND280. These spectra were made using Monte Carlo simulations. They have been normalized to 5×10^{21} POT (protons on target), which corresponds to running the beam for 5 years at full intensity with the maximum proton energy (50 GeV), and represent all neutrinos that impinge upon either detector.

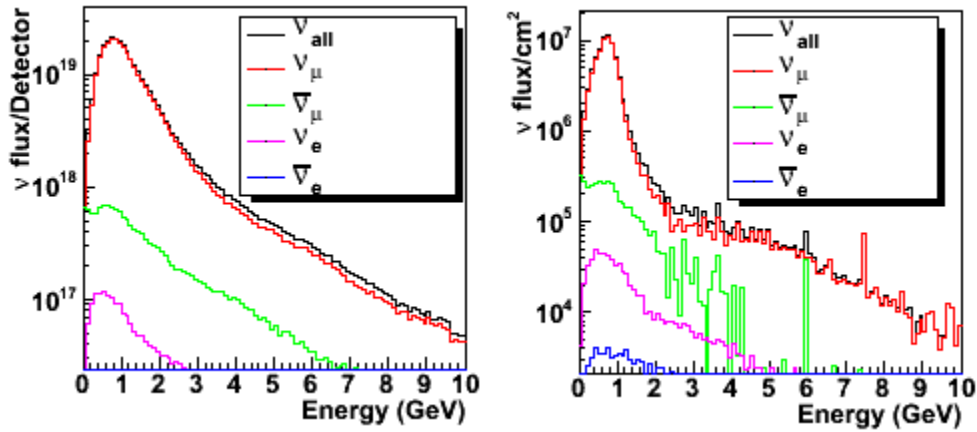


Figure 5.3: Expected energy spectra for neutrinos according to type ND280 (left) and Super K (right). These spectra were made using Monte Carlo simulations. They have been normalized to 5×10^{21} POT (protons on target), which corresponds to running the beam for 5 years at full intensity with the maximum proton energy (50 GeV), and represent all neutrinos that impinge upon either detector.

Figure 5.3 shows the majority of neutrinos resulting from the initial proton beam are muon type neutrinos which result from pion decay. This is an anomaly in the sense that particles generally prefer to decay into the lightest particles possible. Since electrons are lighter than muons, one would expect that pions would decay into an electron and an electron neutrino. However this is not the case for the pion. Since the pion has zero spin, the electron and the antineutrino must emerge with opposite spins or equal helicity/handedness (the projection of spin onto the direction of momentum). An antineutrino is always observed to be right-handed. Therefore, the electron

would also have to be right-handed, but if the electron were massless (which for our purpose is equivalent to saying that it is simply much lighter than the muon), it would only be allowed to exist as a left-handed particle. Therefore, this type of decay is heavily suppressed [3].

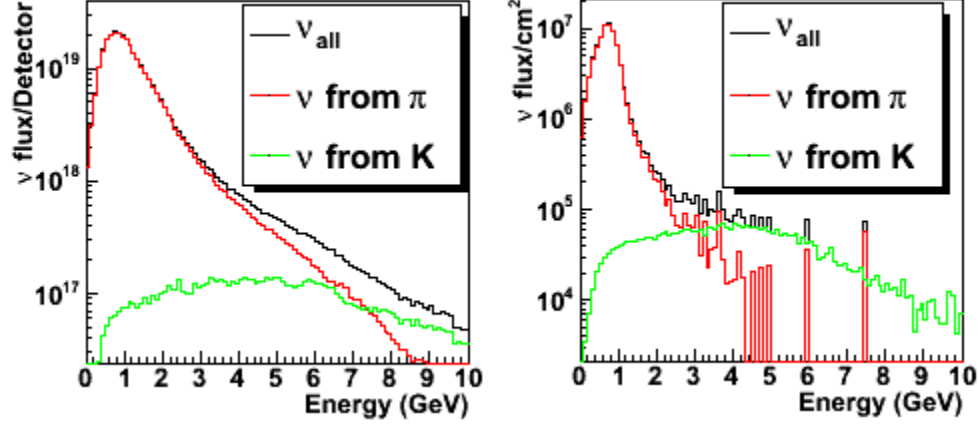


Figure 5.4: Expected energy spectra for neutrinos according to parent particle ND280 (left) and Super K (right). These spectra were made using Monte Carlo simulations. They have been normalized to 5×10^{21} POT (protons on target), which corresponds to running the beam for 5 years at full intensity with the maximum proton energy (50 GeV), and represent all neutrinos that impinge upon either detector.

Figure 5.4 illustrates that the energy of neutrinos resulting from kaons is consistently higher than the energy of neutrinos resulting from pions. As it turns out, this is a relativistic effect which is a result of the fact that kaon's mass (493.7 MeV) is greater than that of the pion (139.6 MeV), combined with the fact that the lifetime of the pion (2.60×10^{-8} s) is about twice as long as the lifetime of the kaon (1.24×10^{-8} s). If it is assumed that the pions and kaons have identical energy spectra (energy due to rest mass plus relativistic kinetic energy) once they leave the graphite target, then it follows that pions have a greater kinetic energy (due to their smaller rest mass energy). Therefore, pions are traveling faster and lasting longer, indicating that they have a greater probability of reaching the end of the decay tunnel before they decay into neutrinos. If a particle reaches the end of the decay tunnel, it will hit dirt, since the decay tunnel is underground. The probability that the particle will interact with the dirt is greater than the probability that the particle will decay into a neutrino and a charged lepton partner. Therefore, the higher energy pions are more likely to reach the end of the decay tunnel and interact with the dirt. In contrast, higher energy kaons are moving slower and lasting for a shorter period of time, so they are decaying into higher energy neutrinos that are eventually being seen by the detectors.

6. Neutrino Interaction Vertices

Figure 6.1 shows the number of events that impinge on the detector due to all neutrino types. The number for the near detector without making reductions of any kind is 2.9×10^{20} and corresponds to all neutrino events from the original beam that actually impinge upon the near detector. However, a reduction must be made to include the interaction cross section, which corresponds to the probability that the neutrino will interact with the material inside the detector as opposed to passing straight through it. It was assumed that the volume of ND280 consisted of the basket only (9 square meters) and was made entirely of plastic (polystyrene). One must also take into account the efficiency of the detector, because the detector will not be able to detect every single neutrino interaction. Since ND280 is a newly built detector, the efficiency has not yet been accurately determined. However, information from computer simulations has led us to believe that the efficiency will be around 90-95%. The cross section for charged current quasi elastic interactions is on the order of 10^{-38} cm^2 , and the efficiency of the near detector is taken to be 90% [4]. Using the cross section approximation for the near detector,

$$(N_b)(\nu \text{ flux})(\sigma)(\epsilon) = N$$

where N = number of events detected, σ = cross section for CCQE interactions (10^{-38} cm^2), ϵ = efficiency (0.9), and N_b = number of target nuclei. In order to calculate N_b , I used

$$N_b = (\rho)(V)(1/M)(N_A)(a),$$

where V = Volume (111 m^3), M = molar mass of plastic (0.105 kg/mol), ρ = density of plastic (1050 kg/m^3), a = number of target nuclei per mole (16), and N_A = Avogadro's number.

$$(1.06 \times 10^{31} \text{ nuclei})(2.9 \times 10^{20} \nu / (9 \times 10^4 \text{ cm}^2))(10^{-38} \text{ cm}^2)(.90) = 3 \times 10^8 \nu \text{ events}$$

After using this information, the number of events that the detector actually sees is reduced to 3×10^8 .

Figure 6.1 shows that there is a distinctive asymmetry in the distributions of neutrino interaction vertices associated with ND280. The asymmetry corresponds to a greater number of events being seen in the most positive x/most negative y coordinates. Figure 6.2 shows the ratio of events seen at a specific position normalized to the number of events seen by the center of ND280. It shows that there are approximately 30% more hits in the most positive x and most negative y direction than in the center. This can be attributed to the fact that ND280 is located 2.5 degrees off axis.

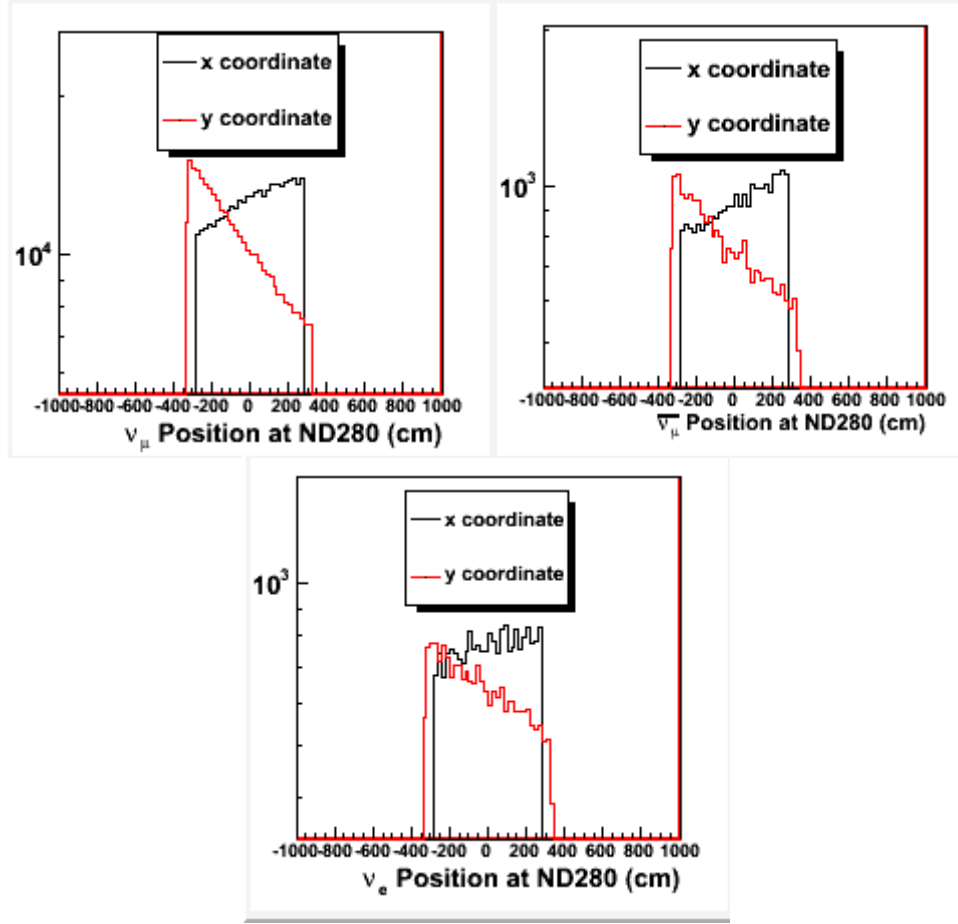


Figure 6.1: The distributions as seen by ND280 for all neutrino types in the detector coordinates { muon neutrinos (top left), antimuon neutrinos (top right), and electron neutrinos (bottom)}. The x coordinate corresponds to the horizontal direction across the detector; the y coordinate corresponds to the vertical component of the detector. These plots were made using Monte Carlo simulations. They have been normalized to 5×10^{21} POT (protons on target), which corresponds to running the beam for 5 years at full intensity with the maximum proton energy (50 GeV), and represent all neutrinos that impinge upon ND280.

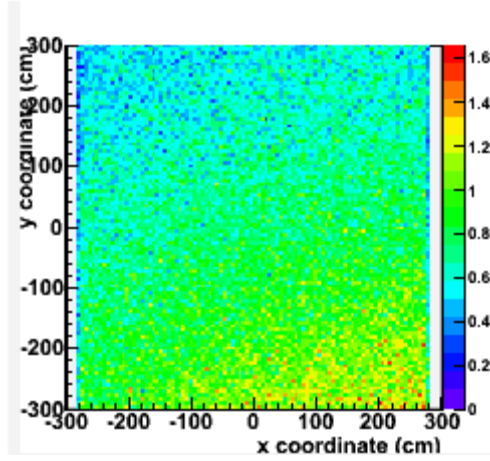


Figure 6.2 A plot that shows the ratio of events as seen by the center of ND280 to all other events as seen by ND280. This plot was made using Monte Carlo simulations. It has been normalized to 5×10^{21} POT (protons on target), which corresponds to running the beam for 5 years at full intensity with the maximum proton energy (50 GeV).

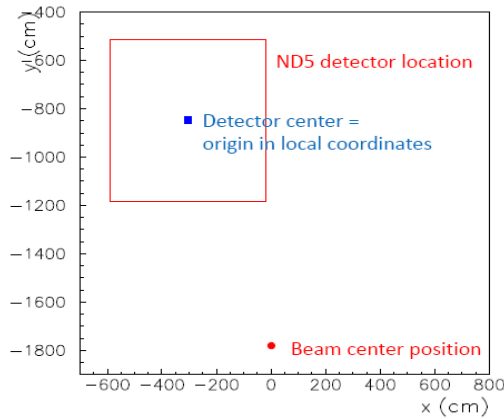


Figure 6.3: The location of ND280 with respect to the initial proton beam

Figure 6.3 shows the location of ND280 with respect to the center of the initial proton beam and neutrino beam. Since most of the particles are concentrated near the center of the beam after being focused by the magnetic horns, the majority of hits seen by ND280 are in the most positive x (which is illustrated by the right side of the detector in Figure 6.3) and most negative y direction (which is illustrated by the bottom of the detector in Figure 6.3). Having the highest number of neutrinos in the center of the detector would correspond to an on axis detector.

Figures 6.1 and 6.2 could be useful tools in monitoring the off axis angle once T2K is running at full intensity. The asymmetry seen in the neutrino interaction vertices reveals where the highest concentrations of neutrinos are with respect to the detector center. Monitoring the off axis angle will be crucial once the experiment is running because it is what is responsible for the peak in the

energy spectra (see Figure 5.1). Since the probability formulas have a dependence on L/E , accurately measuring the energy spectra is imperative to accurately measuring θ_{13} .

7. Detector Interactions

Using Monte Carlo simulations, it is possible to project the types of neutrino interactions ND280 will see after 5 years. These interactions were simulated using the entire volume of the detector (all subdetectors including SMRD), but assume that the POD water molecules are filled with air instead of water. After simulating 5 years of running at full intensity, it is expected that the neutrino beam will produce $\sim 10^8$ interactions in ND280. Of these interactions, approximately 28% will be neutral current interactions, and 72% will be charged current interactions. 38% of the total interactions will be CCQE interactions. 13% of the total interactions will involve a π^0 (8.5% of which will be charged current interactions and 4.5% will be neutral current interactions). The interactions that involve π^0 's will become important when discussing sources of electron neutrino background.

8. Muon Neutrino Disappearance

Using the approximate probability that a muon neutrino will remain a muon neutrino

$$P(\nu_\mu \rightarrow \nu_\mu) = 1 - \sin^2 2\theta_{23} \sin^2(1.27 \Delta m_{23}^2 L/E),$$

an energy spectrum including the muon neutrino disappearance can be constructed. In the following graphs, the red curve uses the best current measurements for the parameters in the oscillation formula which are 1 for $\sin^2 2\theta_{23}$ and 2.5×10^{-3} for Δm_{23}^2 [7].

The left figure in Figure 8.1 shows the energy spectrum for Super K, assuming no oscillations have taken place. It also shows the spectrum that Super K should actually measure, accounting for oscillations via the disappearance of muon neutrinos. However, what is mainly of interest in trying to find a limit on θ_{23} , is the ratio of the non oscillated spectrum to the oscillated spectrum.

Using the cross section approximation, the fact that the fiducial volume of Super K is 22.5 kilotons [10], and is composed of water,

$$(N_b)(\nu \text{ flux})(P)(\sigma)(\epsilon) = N$$

where N = number of events detected, σ = cross section for CCQE interactions (10^{-38}cm^2), ϵ = efficiency (0.99), $P = P(\nu_\mu \rightarrow \nu_\mu) = 1 - \sin^2 2\theta_{23} \sin^2(1.27 \Delta m_{23}^2 L/E)$, and N_b = number of target nuclei.

In order to calculate N_b I used,

$$N_b = (m)(1/M)(N_A)$$

where m = fiducial mass (2.25×10^7 kg), M = molar mass of water (0.018 kg/mol), and N_A = Avogadro's number.

$$(7.5 \times 10^{32} \text{ nuclei})(7.29 \times 10^7 \nu_\mu \text{ flux})(10^{-38} \text{ cm}^2)(.99) = 541 \nu_\mu \text{ events (ignoring oscillations)}$$

$$(7.5 \times 10^{32} \text{ nuclei})(2.2 \times 10^7 \nu_\mu \text{ flux})(10^{-38} \text{ cm}^2)(.99) = 163 \nu_\mu \text{ events (account for oscillations)}$$

After plugging in the appropriate numbers, there are 541 muon neutrino events expected if neutrino oscillations are ignored, and 163 muon neutrino events expected after neutrino oscillations are taken into account. If the previous two numbers are subtracted, there are 378 fewer events expected after oscillations of muon neutrinos are taken into account as compared to ignoring oscillations.

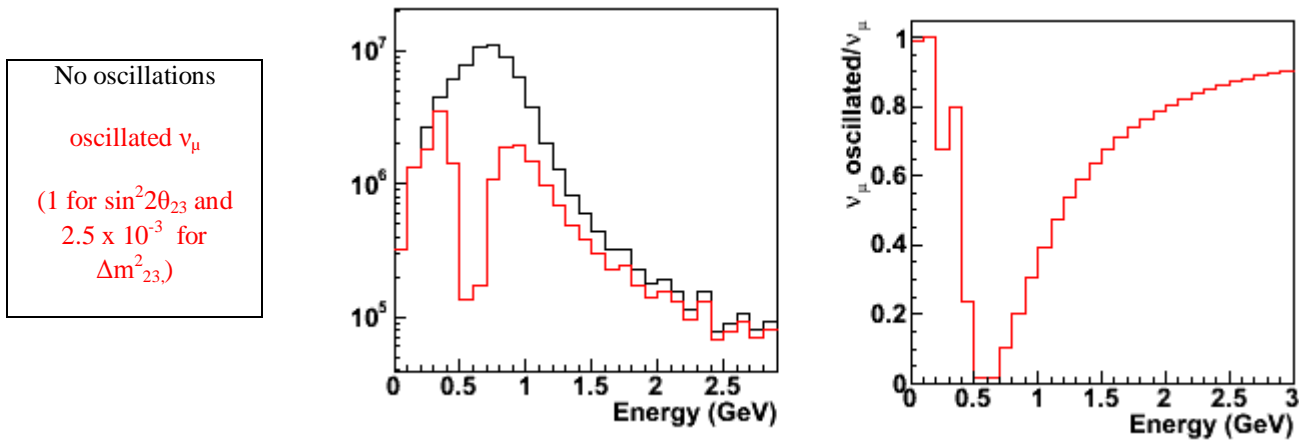


Fig 8.1: The energy spectra as seen by Super K with and without muon neutrino disappearance (left). The ratio of the oscillated spectrum to the non-oscillated spectrum (right). These spectra were made using Monte Carlo simulations. They have been normalized to 5×10^{21} POT (protons on target), which corresponds to running the beam for 5 years at full intensity with the maximum proton energy (50 GeV). The default values used in the spectrum with oscillations are 1 for $\sin^2 2\theta_{23}$ and 2.5×10^{-3} for Δm^2_{23} .

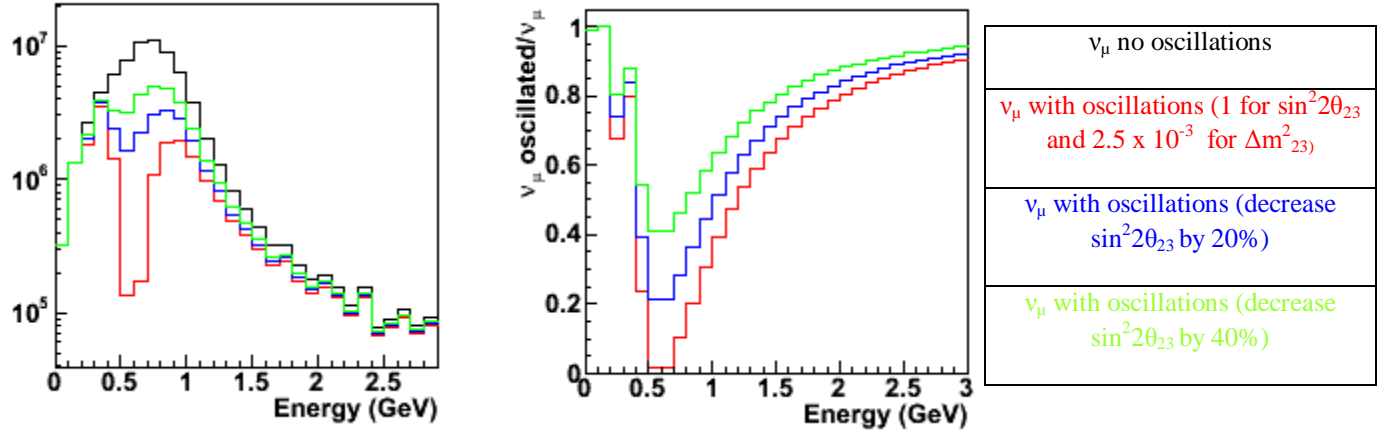


Figure 8.2: The energy spectra for the graphs at Super K with and without oscillations (left). The ratio of the oscillated spectrum to the non-oscillated spectra (right). These spectra were made using Monte Carlo simulations. They have been normalized to 5×10^{21} POT (protons on target), which corresponds to running the beam for 5 years at full intensity with the maximum proton energy (50 GeV). The default values used in the spectrum with oscillations are 1 for $\sin^2 2\theta_{23}$ and 2.5×10^{-3} for Δm^2_{23} .

Figure 8.2 shows how the oscillated spectra and the ratio of the oscillated to non-oscillated energy spectra vary as the value of the parameter $\sin^2 2\theta_{23}$ decreases. As it decreases, the size of the dip seen in the energy spectra decreases. Hence, the dip in the plot of the ratio of energy spectra becomes less pronounced as $\sin^2 2\theta_{23}$ decreases. These plots will be very useful when data has been acquired in order to put a limit on $\sin^2 2\theta_{23}$.

Figure 8.3 shows how the energy spectra changes if the value of the parameter Δm^2_{23} is increased or decreased. If Δm^2_{23} is increased, the right side of the oscillated energy spectra decreases. Also, the dips in the ratios of energy spectra are shifted to a higher energy. If Δm^2_{23} is decreased, the left side of the oscillated energy spectra decreases. Also, the dips in the ratios of energy spectra are shifted to lower energies.

Therefore, the position of the dip in the ratios of the energy spectra can help determine the value of Δm^2_{23} , and information about the value of $\sin^2 2\theta_{23}$ is determined by the depth of the peak of the ratio spectrum.

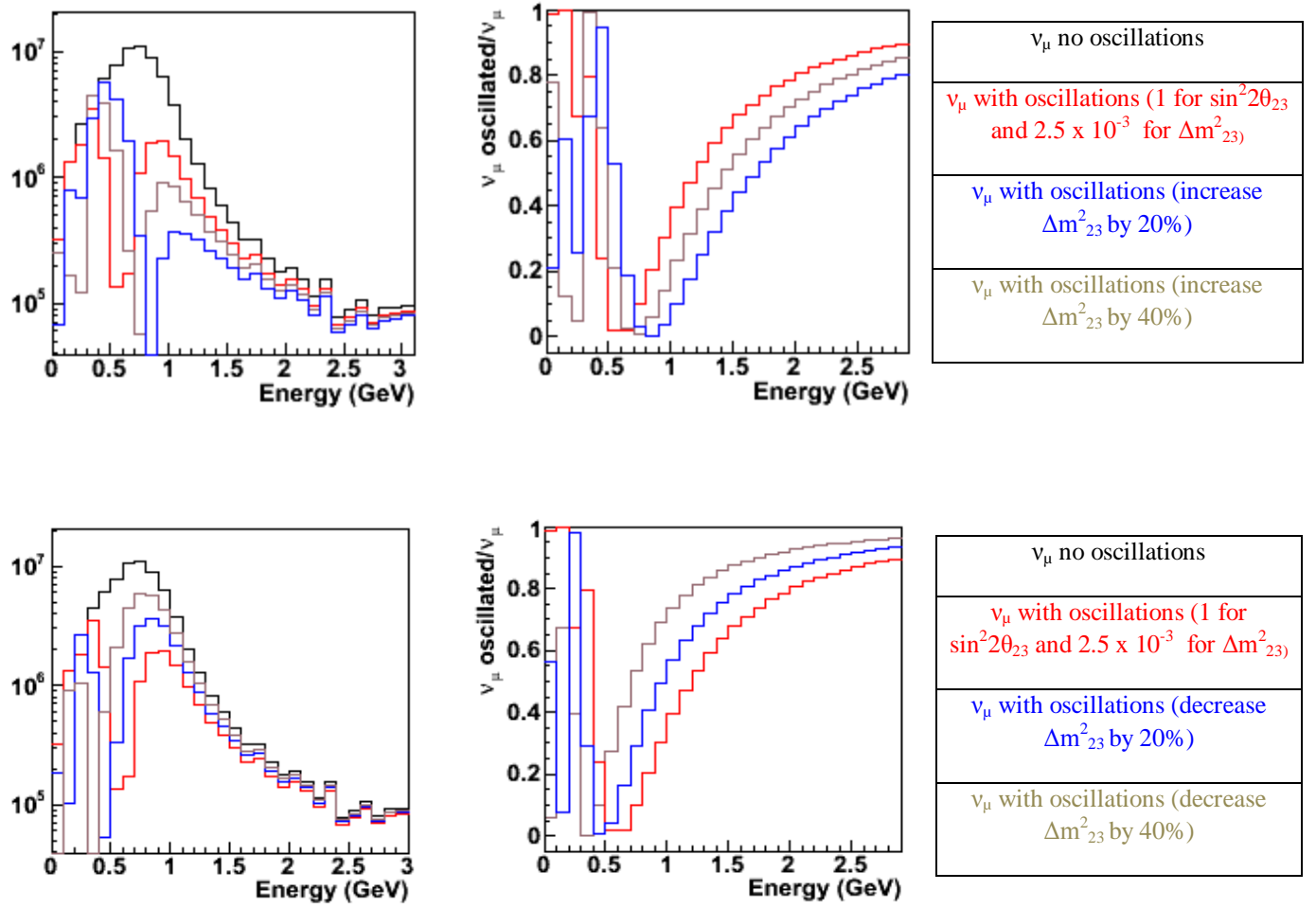


Figure 8.3: The energy spectra for the graphs at Super K with and without oscillations (left). The ratio of the oscillated spectrum to the non-oscillated spectra (right). These spectra were made using Monte Carlo simulations. They have been normalized to 5×10^{21} POT (protons on target), which corresponds to running the beam for 5 years at full intensity with the maximum proton energy (50 GeV). The default values used in the spectrum with oscillations are 1 for $\sin^2 2\theta_{23}$ and 2.5×10^{-3} for Δm^2_{23} .

9. Electron Neutrino Appearance

Using the approximate probability that a muon neutrino will oscillate into an electron neutrino:

$$P(\nu_\mu \rightarrow \nu_e) = \sin^2 \theta_{23} \sin^2 2\theta_{13} \sin^2(1.27 \Delta m^2_{23} L/E),$$

the following plots simulating the energy spectra of electron neutrinos resulting from oscillations can be constructed. In these plots, the red (oscillated) curve uses the best current measurements for the values for the parameters in the oscillation formula which are 0.5 for $\sin^2 \theta_{23}$ and 2.5×10^{-3} for Δm^2_{23} . There is only an upper limit known for $\sin^2 2\theta_{13}$, so it was assumed to be 0.1 [7].

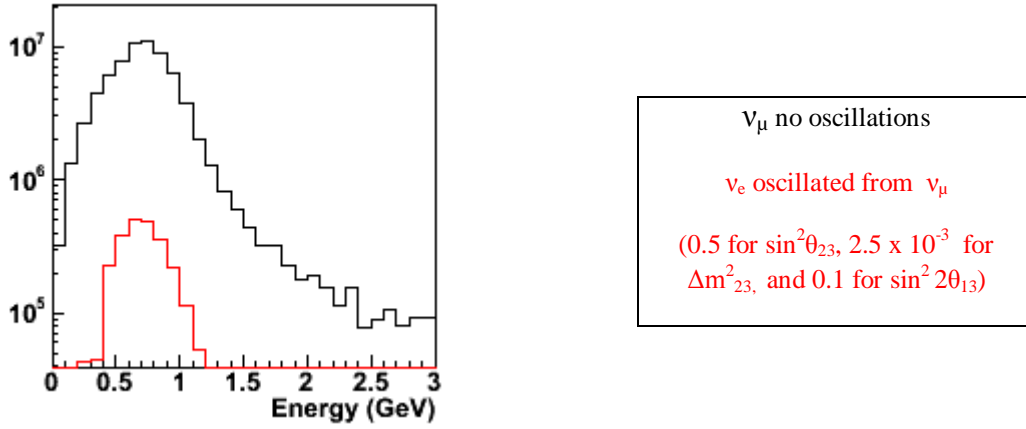


Figure 9.1: The expected energy spectrum for all muon neutrinos and electron neutrinos oscillating from muon neutrinos. These spectra were made using Monte Carlo simulations. They have been normalized to 5×10^{21} POT (protons on target), which corresponds to running the beam for 5 years at full intensity with the maximum proton energy (50 GeV). The default values used in the spectrum with oscillation are 0.5 for $\sin^2 \theta_{23}$, 2.5×10^{-3} for Δm^2_{23} , and 0.1 for $\sin^2 2\theta_{13}$.

Figure 9.1 shows the energy spectrum that is expected due to electron neutrinos which oscillate from muon neutrinos. Using a cross section approximation, the fact that the fiducial volume of Super K is 22.5 kilotons, and is composed of water,

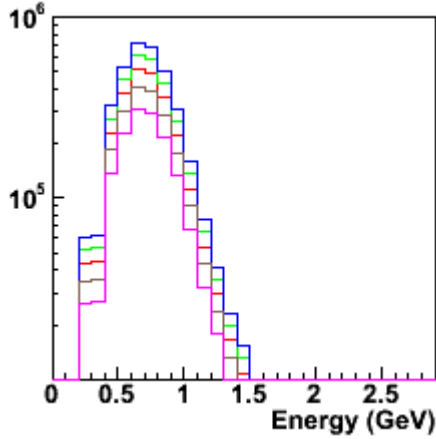
$$(N_b)(\nu \text{ flux})(P)(\sigma)(\epsilon) = N$$

where N = number of events detected, σ = cross section for CCQE interactions (10^{-38} cm^2), ϵ = efficiency (0.99), $P = P(\nu_\mu \rightarrow \nu_e) = \sin^2 \theta_{23} \sin^2 2\theta_{13} \sin^2(1.27 \Delta m^2_{23} L/E)$, and N_b = number of target nuclei (7.5×10^{32} nuclei).

$$(7.5 \times 10^{32} \text{ nuclei})(2.53 \times 10^6 \nu_e/\text{cm}^2)(10^{-38} \text{ cm}^2)(.99) = 19 \nu_e \text{ events}$$

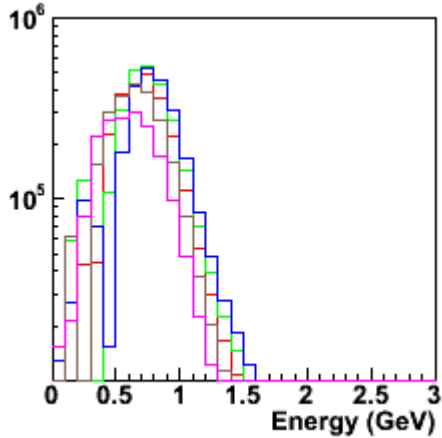
After plugging in the appropriate numbers, 19 electron neutrino events are expected due to oscillation if $\sin^2 2\theta_{13}$ is 0.1.

Figure 9.2 shows how the energy spectrum for electron neutrinos expected from oscillations changes as the parameter $\sin^2 2\theta_{13}$ is decreased or increased. As $\sin^2 2\theta_{13}$ is increased, the energy spectra are shifted upward, and more electron neutrinos are seen. Likewise, as $\sin^2 2\theta_{13}$ is decreased, the energy spectra are shifted downward, and fewer electron neutrinos are seen.



ν_e oscillated from ν_μ (0.5 for $\sin^2\theta_{23}$, 2.5×10^{-3} for Δm^2_{23} , and 0.1 for $\sin^2 2\theta_{13}$)
ν_e oscillated (increase $\sin^2 2\theta_{13}$ by 20%)
ν_e oscillated (increase $\sin^2 2\theta_{13}$ by 40%)
ν_e oscillated (decrease $\sin^2 2\theta_{13}$ by 20%)
ν_e oscillated (decrease $\sin^2 2\theta_{13}$ by 40%)

Figure 9.2: Illustration of how the electron neutrino energy spectra expected from oscillations varies as $\sin^2 2\theta_{13}$ is increased or decreased. These spectra were made using Monte Carlo simulations. They have been normalized to 5×10^{21} POT (protons on target), which corresponds to running the beam for 5 years at full intensity with the maximum proton energy (50 GeV). The values used for all spectra are 0.5 for $\sin^2\theta_{23}$, 2.5×10^{-3} for Δm^2_{23} , and the default value for $\sin^2 2\theta_{13}$ is 0.1.



ν_e oscillated from ν_μ (0.5 for $\sin^2\theta_{23}$, 2.5×10^{-3} for Δm^2_{23} , and 0.1 for $\sin^2 2\theta_{13}$)
ν_e oscillated (increase Δm^2_{23} by 20%)
ν_e oscillated (increase Δm^2_{23} by 40%)
ν_e oscillated (decrease Δm^2_{23} by 20%)
ν_e oscillated (decrease Δm^2_{23} by 40%)

Figure 9.3: Illustration which shows how the energy spectra of electron neutrinos expected from oscillations varies as Δm^2_{23} is increased or decreased. These spectra were made using Monte Carlo simulations. They have been normalized to 5×10^{21} POT (protons on target), which corresponds to running the beam for 5 years at full intensity with the maximum proton energy (50 GeV). The default values used for the spectrum with oscillation are 0.5 for $\sin^2\theta_{23}$, 2.5×10^{-3} for Δm^2_{23} , and 0.1 for $\sin^2 2\theta_{13}$.

Figure 9.3 shows how the energy spectra for electron neutrinos change as the parameter Δm^2_{23} is varied. The effect is very similar to that for the muon neutrino disappearance. Increasing Δm^2_{23}

causes the energy spectra to be shifted into areas of slightly higher energy, whereas decreasing Δm_{23}^2 causes the energy spectra to be shifted into areas of slightly lower energy.

10. Electron Neutrino Background

T2K is designed to search for the appearance of electron neutrinos in an almost pure beam of muon neutrinos. However, some electron neutrino background is unavoidable. Therefore, it is imperative that these sources of background be minimized, if possible, and well understood. In the T2K experiment, there are two dominant sources of background to the electron neutrino signal. The first major source of electron neutrino background consists of those that are intrinsic to the original neutrino beam. Once the neutrino beam reaches the near detector, it is assumed that no oscillations have taken place since the beam has only propagated 280 meters. However, there are still some electron neutrinos located in the beam. These electron neutrinos result from the decay of kaons and muons. Those that decay from kaons generally possess a higher energy than those that decay from muons. These events are unavoidable, but the near detector will be able to measure the energy spectrum of these electron neutrinos and approximately how many there are. Using Figure 10.1 along with a cross section approximation, it is possible to estimate the number of intrinsic electron neutrinos. It was assumed that the volume of the near detector simply included the basket (all subdetectors with the exception of SMRD), which has an effective area of 9 square meters. It was also assumed that the detector was made entirely of plastic. While this is an oversimplified version of the detector, the number of events should be correct to within an order of magnitude. Using the cross section approximation for the near detector (see section 6):

$$(N_b)(\nu \text{ flux})(\sigma)(\epsilon) = N$$

where N = number of events detected, σ = cross section for CCQE interactions (10^{-38} cm^2), ϵ = efficiency (0.9), and N_b = number of target nuclei (1.06×10^{31} nuclei).

$$(1.06 \times 10^{31} \text{ nuclei})(2.2 \times 10^{18} \nu_e / (9 \times 10^4 \text{ cm}^2))(10^{-38} \text{ cm}^2)(.90) = 2.3 \times 10^6 \nu_e \text{ events}$$

After this approximation, there are $\sim 10^6$ electron neutrino events which will be seen at the near detector. For Super K, the fiducial volume of 22.5 kilotons was used [10], and that it is made entirely of water.

$$(N_b)(\nu \text{ flux})(P)(\sigma)(\epsilon) = N$$

where N = number of events detected, σ = cross section for CCQE interactions (10^{-38} cm^2), ϵ = efficiency (0.99), $P = P(\nu_\mu \rightarrow \nu_e) = \sin^2 \theta_{23} \sin^2 2\theta_{13} \sin^2(1.27 \Delta m_{23}^2 L/E)$, and N_b = number of target nuclei (7.5×10^{32} nuclei).

$$(7.5 \times 10^{32} \text{ nuclei})(7.1 \times 10^5 \nu_e / \text{cm}^2)(10^{-38} \text{ cm}^2)(.99) = 5 \nu_e \text{ events}$$

The estimated number of events is ~ 5 electron neutrino events visible at the far detector.

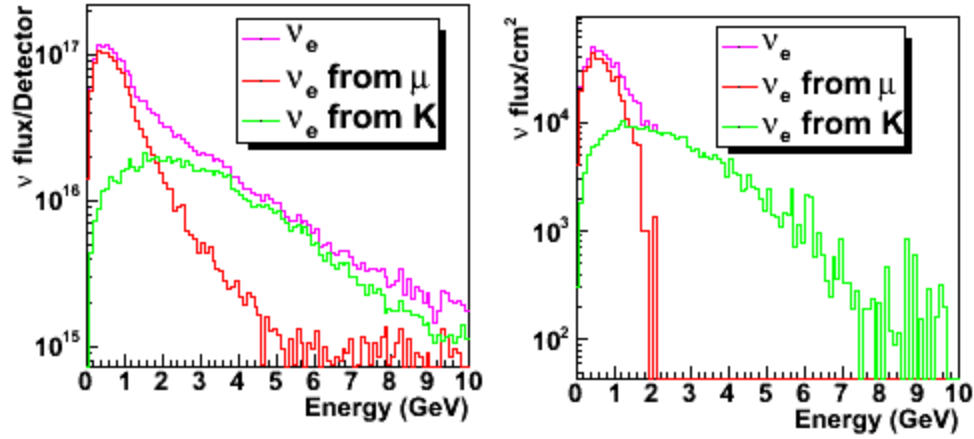


Figure 10.1: The energy spectrum for electron neutrinos at ND280 (right) and Super K (left). These spectra were made using Monte Carlo simulations. They have been normalized to 5×10^{21} POT (protons on target), which corresponds to running the beam for 5 years at full intensity with the maximum proton energy (50 GeV), and represent all neutrinos that impinge upon either detector.

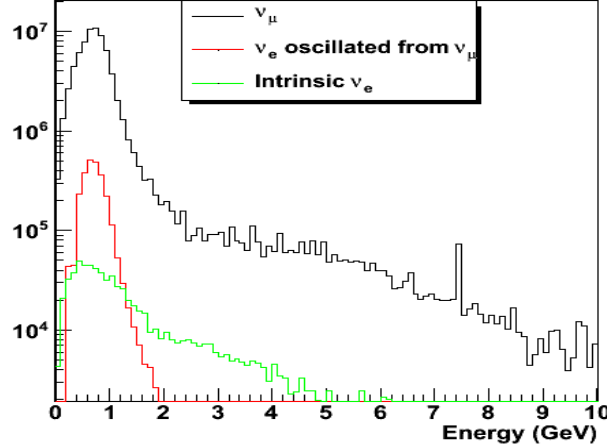


Figure 10.2: The energy spectra for muon neutrinos, electron neutrinos intrinsic to the original neutrino beam, and those electron neutrino events expected due to oscillation. These spectra were made using Monte Carlo simulations. They have been normalized to 5×10^{21} POT (protons on target), which corresponds to running the beam for 5 years at full intensity with the maximum proton energy (50 GeV).

Figure 10.2 shows the energy spectra for muon neutrinos, electron neutrinos intrinsic to the original beam, and those electron neutrino events expected due to oscillation. It can be seen that the electron neutrinos expected from oscillations are peaked in the energy range from 0-2 GeV

whereas the intrinsic electron neutrino events have a tail that extends into areas of higher energy. This will be very useful when analyzing events from Super K since those that have a higher energy can be disregarded as background electron neutrinos. After these higher energy events have been discarded, there are ~ 4 intrinsic electron neutrino events expected at the far detector.

It is not necessary to include calculations that are based on intrinsic electron neutrinos oscillating into other kinds of neutrinos because this number is very small. After using the approximate electron neutrino survival probability

$$P(\nu_e \rightarrow \nu_e) = 1 - \sin^2 2\theta_{13} \sin^2(1.27 \Delta m_{23}^2 L/E),$$

it is expected that there will be 0.8 neutrino events expected from oscillations of intrinsic electron neutrinos after 5 years of running at full intensity. It will not enter into the calculation of electron neutrinos oscillated from muon neutrinos because it will be hidden by other, larger uncertainties.

The next major source of electron neutrino background comes from neutral current events which produce a π^0 . The π^0 then decays into two photons. However, if these neutral current interactions occur within Super K, these photons have an energy comparable to that of an electron neutrino. Therefore, the photons can collide with the electrons in the water molecules of Super K and produce an event that is read out by the PMT's of Super K. If these two photons have a relatively small angle between them, then the PMT's of Super K will not be able to resolve the difference between the effects of one photon or two photons, possibly causing that event to be mislabeled as an event caused by an electron neutrino.

Using Monte Carlos simulations, it is expected that $\sim 10^6$ neutral current events involving a π^0 will be observed after 5 years at ND280. Only ~ 10 of these will be mislabeled as electron neutrino events at Super K [15].

While the events related to electron neutrino background will constitute a small portion of the events seen by the near and far detectors, it is imperative that they are measured accurately. There are only ~ 19 electron neutrino events expected from oscillations, which is a very small pool of events with which to work when compared to a relatively large background. Therefore, in order to be able to successfully extract the oscillation events from these backgrounds, the backgrounds must be carefully studied and understood.

11. Extracting θ_{13} and Δm_{23}^2

After all the previous data has been collected, one is left with the question of how to measure the various parameters T2K has been designed to find. To accomplish this, the data set that is actually collected from Super K is compared to various simulated data sets in order to determine which simulated data fits the actual data best.

It is possible to test the efficiency of various fitting method by testing them on a “fake” data set. The fake data set consisted of the probability that a muon neutrino will oscillate into an electron neutrino as a function of energy. Using the probability formula for electron neutrino appearance [2],

$$P(\nu_\mu \rightarrow \nu_e) = \sin^2\theta_{23} \sin^2 2\theta_{13} \sin^2(1.27\Delta m_{23}^2 L/E),$$

a function was defined to step through various values for $\sin^2 2\theta_{13}$ and Δm_{23}^2 . The minimization routine (MINUIT) then fit these simulated data to the fake data set and calculated the uncertainty (or χ^2) associated with the fit.

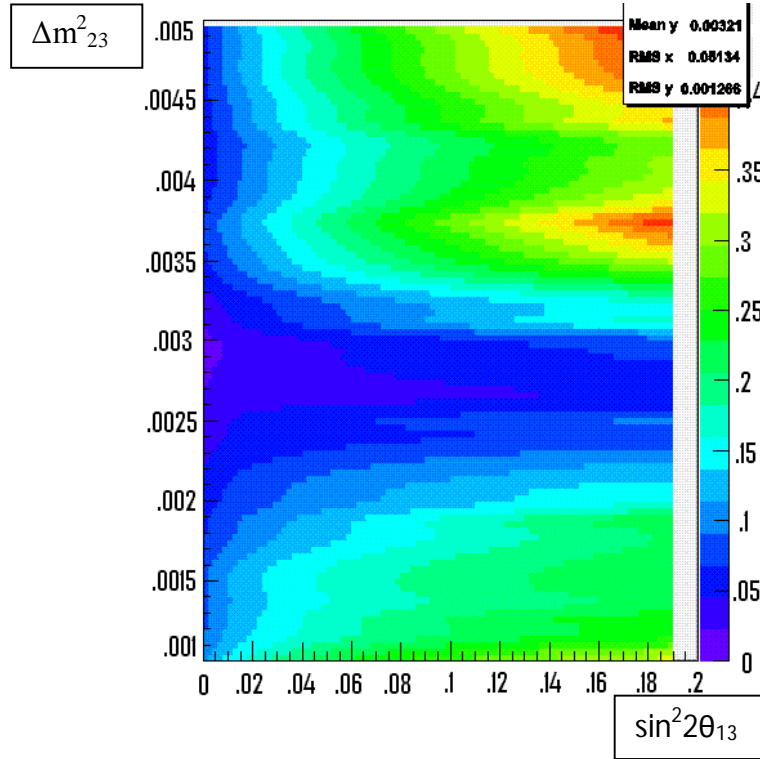


Figure 11.1: Illustration showing the best fit for the parameters $\sin^2 2\theta_{13}$ and Δm_{23}^2

Figure 11.1 shows the best fits for the parameters $\sin^2 2\theta_{13}$ and Δm_{23}^2 are in the violet region where the values for the uncertainties are the lowest. The values corresponding to the fits in the violet region are $0 \leq \sin^2 2\theta_{13} \leq 0.14$ and $2.4 \times 10^{-3} \leq \Delta m_{23}^2 \leq 3.3 \times 10^{-3}$.

However, there is not much useful information about $\sin^2 2\theta_{13}$, since all values up to 0.2 result in relatively good fits. However more iterations can be done in order to better the minimization routine and extracting more useful values. In addition, Figure 11.1 does not account for any sources of electron neutrino background. In the future these would have to be included in order to extract useful information about $\sin^2 2\theta_{13}$ and Δm_{23}^2 .

12. Summary

In summary, T2K has been designed to search for electron neutrino appearance in a beam of muon neutrinos. When these neutrinos are actually measured, the number of neutrinos that interact with the material inside the detector will be drastically smaller than the number of neutrinos that impinge upon the detector. The number of events expected to be seen at the near detector, after taking into account the approximate interaction cross section, is $\sim 10^8$ for ND280. Also, the efficiency of the detector must be taken into account. Even though a certain number of neutrinos will interact with the detector, the detector's inability to identify every event will also decrease the number of events that can eventually be used for data analysis.

There is also an asymmetry in the distribution of neutrino interaction vertices seen by the near detector. The majority of neutrinos are seen in the most positive x/negative y coordinate which is due to the fact that our detector is located 2.5 degrees off axis with respect to the original beam. The asymmetry seen in the distribution of the neutrino interaction vertices of ND280 could be a very useful tool in monitoring the off axis angle.

Using Monte Carlo simulations, it is possible to project what interactions ND280 will see after 5 years. After simulating 5 years of running at full intensity, it is expected that the neutrino beam will produce $\sim 10^8$ interactions in ND280. Of these interactions, the majority are CCQE interactions.

T2K will measure the deficit of muon neutrinos in order to place better limits on θ_{23} and Δm_{23}^2 . The parameter Δm_{23}^2 can be measured by the location of the energy of the peak in the electron neutrino spectrum. For the muon neutrino spectra, it gives information about the location of the dip in the ratio of the oscillated to the non-oscillated energy spectra. The parameter θ_{23} is determined by how many muon neutrinos will oscillate into other flavors of neutrinos. 70% fewer muon neutrino CCQE events will be observed than would be observed if oscillations did not occur.

The parameter θ_{13} gives information on the percentage of the original muon neutrinos that will oscillate into electron neutrinos. Based on event estimations, there are approximately 19 electron neutrino CCQE events expected at the far detector after 5 years due to neutrino oscillation from muon neutrinos to electron neutrinos.

Once the neutrino beam reaches the near detector, it is important to correctly identify sources of electron neutrino background in order to subtract this number from the electron neutrinos in the final beam. The two major sources of electron neutrino background are electron neutrinos intrinsic to the original beam from kaon and muon decay and those events that could be mislabeled as electron neutrino events because of π^0 decay. From simulated data, it can be estimated that there are $\sim 10^6$ intrinsic electron neutrino events at ND280, and ~ 4 intrinsic electron neutrino events at Super K. If these backgrounds are understood, it will enable T2K to correctly determine the number of electron neutrinos that have specifically oscillated from muon

neutrinos. It is also estimated that ~ 10 events will be mislabeled as electron neutrino events due to π^0 decay.

	Events Expected	
Expected Muon Neutrinos (No Oscillations)	541	
Expected Muon Neutrinos (With Oscillations)	163	
Muon Neutrino Disappearance	378	
Electron Neutrino Appearance	19	
Intrinsic Electron Neutrino Background		4
π^0 Background		10

Table 12.1: Summary of event estimations at Super K

The event numbers recorded in Table 12.1 are somewhat lower as compared to earlier studies which have been performed by the T2K collaboration. Also, Figure 5.2 (the ratio of the far energy spectra/near energy spectra) seems somewhat distorted compared to earlier studies that have been done. I suspect that both of these effects may indicate that the weighting mechanism for the spectra at Super K could have been applied incorrectly.

Lastly, it is possible to run a minimization routine on a fake data set in order to test the effectiveness of certain algorithms in extracting these parameters. From a fake data set, the corresponding values are $0 \leq \sin^2 2\theta_{13} \leq 0.14$ and $2.4 \times 10^{-3} \leq \Delta m^2_{23} \leq 3.3 \times 10^{-3}$.

13. Conclusion

In conclusion, the number of intrinsic electron neutrinos that are found in the original beam is on the order of $\sim 10^6$ for ND280 and ~ 5 for Super K. However, if the intrinsic electron neutrinos that have an energy higher than the energy of the electron neutrinos expected from oscillations, the number of intrinsic electron neutrinos at Super K can be reduced to 4. According to studies done at Super K, there are ~ 10 background events expected from π^0 's. The number of electron neutrino events that are expected from oscillations of muon neutrinos is on the order of 19. Both of these event numbers correspond to a beam run of 5 years at full intensity. Since the background signal is relatively large compared to the signal expected from oscillations, the

background measurements that are made must be extremely precise in order to be able to correctly extract the number of events that are due to neutrino oscillations.

References

1. Griffiths, David. *Introduction to Elementary Particles*. John Wiley & Sons. 2004.
2. Mahn, Kendall. "A search for muon neutrino and antineutrino disappearance with the Booster Neutrino Beam." 2009.
3. Perkins, Donald. *Introduction to High Energy Physics*. Cambridge University Press. 2000
4. Fleming, Bonnie. "Neutrino Cross Sections and Scattering Physics."
5. "Proposal for Participation in the T2K Long-baseline Neutrino Oscillation Experiment." 2005.
6. McBryde, Kevin. "Characterization and Optimization of Detector Components and Measurement Procedures for the Near Detector of the T2K Neutrino Long-baseline Experiment." 2008.
7. Itow, Y. , et al. "The JHF-Kamioka Neutrino Project." 2001.
8. "Neutrino Interaction Topologies." 2001. http://www-donut.fnal.gov/web_pages/DONUT/Topologies.html
9. Bahcall, John. "Solving the Mystery of Missing Neutrinos." 2004.
10. Nakamura, K. "Results from Super-Kamiokande and status of K2K." 2001.
11. Alberico, W.M. "Neutrino Oscillations, Masses, and Mixing." 2003.
12. Maltoni, Michele, et.al. "Status of global fits to neutrino oscillations." 2007.
13. Povh, Bogdan, et. Al. *Particles and Nuclei: An Introduction to the Physical Concepts*. Springer. 2008.

14. “J-PARC Neutrino Flux.” <http://jnusrv01.kek.jp/internal/t2k/nubeam/flux>

15. Kaji, H., Kaneyuki, K. “Study of new e/π^0 separation method.” 2009.